

## Introduction

Based on the 9 wavelength absorption and attenuation meter ac-9 (Moore et al, 1992), the ac-spectra (ac-s) offers almost an order of magnitude increase in spectral resolution of in-situ absorption, scattering, and beam attenuation coefficients. The ac-s features the same flow-through system as the ac-9, same size, and excellent stability. The ac-s employs a 25-cm pathlength for effective measurement of the cleanest natural waters. The light source features a linear variable filter with a collimated beam. The absorption side has a reflecting tube and a large area detector, whereas the attenuation side has a non-reflective tube and a collimated detector. The instrument provides an 80+ wavelength output from 400–730 nm with 4 nm steps. Individual filter steps have a FWHM of 15.5 nm. For instrumental details see the poster at this conference by Moore et al.

## ac-s specifications

Mechanical	Weight in air 13 lbs (5.9 kg)
Diameter 4.1 in (10.4 cm)	Weight in water 2.5 lbs (1.1 kg)
Length 31 (79 cm)	
Pressure housing Acetal copolymer	
Optical	Pathlength 10 or 25 cm
Spectral range 400–730 nm	Linearity $\geq 99\%$ R2
Band pass 15 nm/channel	Beam cross-section 8 mm dia. (nominal)
Output wavelengths 80–90	
Resolution 4 nm	
Precision (430–730 nm) $\pm 0.001 \text{ m}^{-1}$ typ.,	
0.003 $\text{m}^{-1}$ max @ 4 Hz; 0.0005 $\text{m}^{-1}$ typ.,	
0.0015 $\text{m}^{-1}$ max @ 1 Hz,	
(400–449 nm) $\pm 0.005 \text{ m}^{-1}$ typ.,	
0.0012 $\text{m}^{-1}$ max @ 4 Hz; $\pm 0.003 \text{ m}^{-1}$ typ.,	
0.006 $\text{m}^{-1}$ max @ 1 Hz; Accuracy $\pm 0.01 \text{ m}^{-1}$ ;	
Dynamic range 0.001–10 $\text{m}^{-1}$	
Electrical	Current draw 0.83 A @ 12 V nominal;
Input 10–35 VDC	Connector MCBH6M
Serial output RS-232, -422, or -485	
Sample rate 4 scans/sec, nominal.	
Environmental	Temperature range 0–30 deg C Depth rating 500 m
Pressure sensor optional	

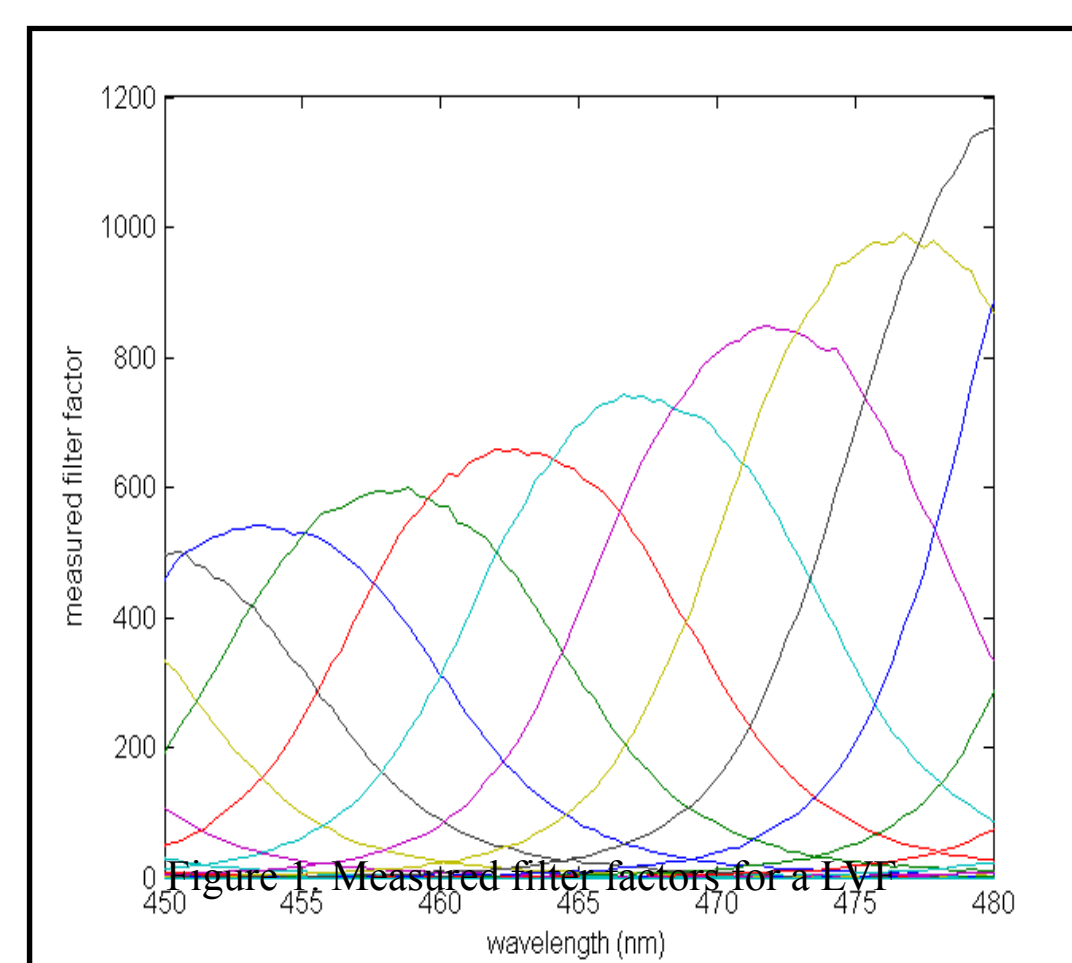


Figure 1. Measured filter factors for a 10 cm pathlength.

The ac-s uses a Linear Variable Filter (LVF) to obtain its wavelengths. The instrument averages 60 individual spectral measurements to report one measurement. The spectrum of each of the 60 individual measurements is determined by the instrument optics and the wavelength. The averaged filter spectra were reported approximately every 4 nm. Figure 1 shows some of these measured filter factors.

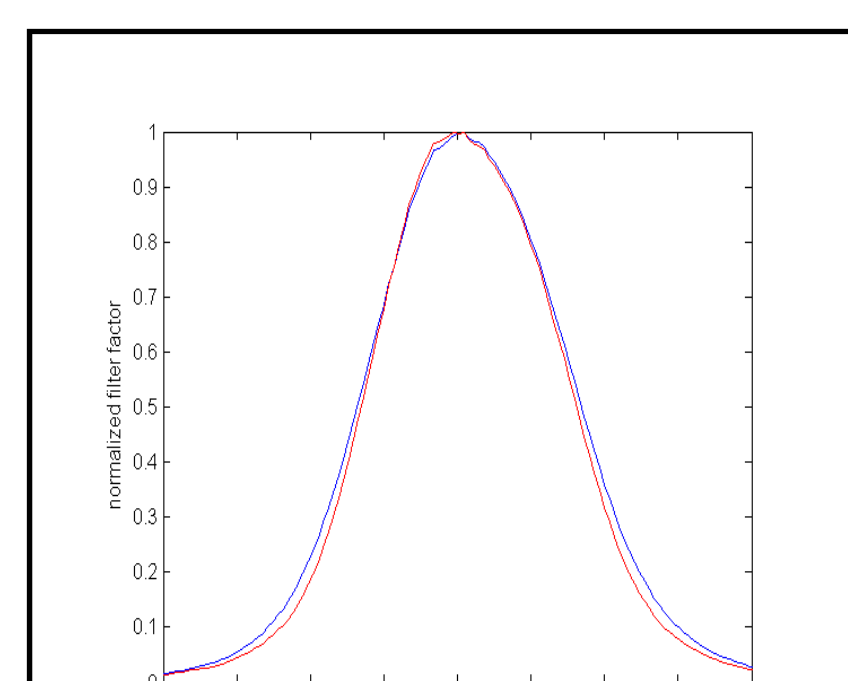


Figure 2. Measured (red) and averaged (blue) filter factors over 60 measurements.

Figure 2 compares a measured filter factor and a calculated one averaged over 60 interpolated steps. Note that the averaged filter is about 2 nm wider.

In order to get the actual filter factor, adjacent filter factors were interpolated into 60 steps. The new filter is the average of 30 of these interpolated filters to either side of the measured filter. This broadens the filter somewhat.

With the filter factors for the ac-s determined, we can predict what the ac-s would measure given an actual spectrum. We normalize the area under each filter, since that is in effect done by the reference detector. Let the normalized filter matrix be given by  $A$ , and the actual spectrum by  $s_a(\lambda)$ , then the measured spectrum,  $s_m(\lambda)$ , will be given by:

$$s_m(\lambda) = A^* s_a(\lambda) \quad (1)$$

An example is shown in figure 3.

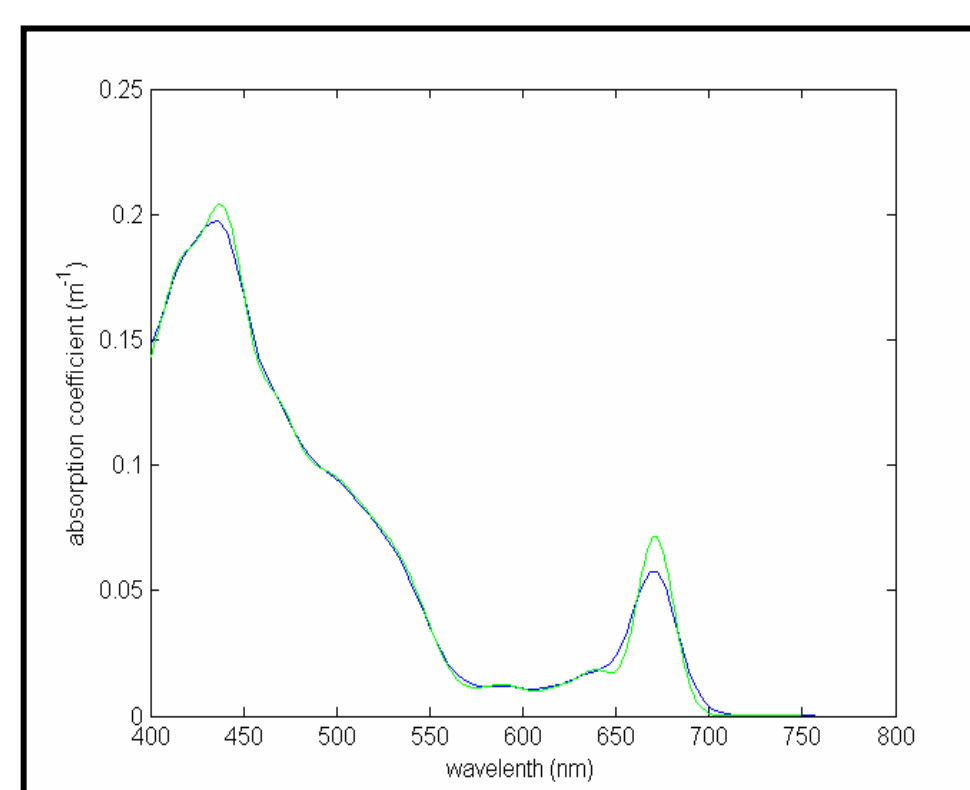


Figure 3. "Actual" (green) and "measured" (blue) absorption spectra for simulated green algae. Note that the ac-s cuts off the peaks and fills in the lows due to averaging. The "actual" spectrum was modeled after an absorption spectrum for green algae found in Fig. 9.4 in Kirk (1994).

## Correction of measured spectra

We now wish to correct the overshoot and undershoot of steeply curved sections of  $a(\lambda)$ . For example the red chlorophyll peak will always be underestimated by any instrument with filters. We note that the ac-s cannot generate curves that are any steeper (more "pointy") than the individual filter factors of the ac-s. If one imagines an absorption spectrum that consists of a delta function at a single wavelength, then several consecutive filter factors will "see" the delta function, resulting in the delta function being rendered as an absorption spectrum with the shape of the filter factor.

The second derivative or the curvature of the actual spectrum is underestimated. We thus generated an ad hoc correction based on the second derivative. Since the red peak is usually the most prominent underestimated feature, we normalized to it. The correction looks as follows:

$$a_c(\lambda) = a_m(\lambda) + 0.17 a_m''(671) [a_m''(\lambda) / a_m''(671)] \quad (2)$$

where  $a_c(\lambda)$  is the corrected absorption spectrum,  $a_m(\lambda)$  is the measured absorption spectrum and  $a_m''(\lambda)$  is the second derivative of the measured absorption spectrum. The factor 0.17 was determined by trial and error. In other words, the correction is a fraction of the absorption at 671 nm. The fraction is determined by the ratio of the local second derivative relative to the second derivative at 671 nm. Applying this correction to the measured (blue) spectrum in Fig. 4, gives the corrected spectrum (red curve) in that figure.

The derivative is a local property. Any noise in the measured absorption spectrum will dominate the derivatives. It is therefore necessary to average prior to determining derivatives. Such averaging may remove signals of interest. The averaging window should thus be kept small enough to average noise, but not so large as to remove signal. We find a window of 10 to 15 nm optimal.

The newly derived spectrum can be convolved with the filter factors as in Eq. (1). This provides a second "measured"  $a_{m2}(\lambda)$  spectrum. A second corrected absorption spectrum is then obtained by adding the difference:

$$a_{c2}(\lambda) = a_c(\lambda) + [a_m(\lambda) - a_{m2}(\lambda)] \quad (3)$$

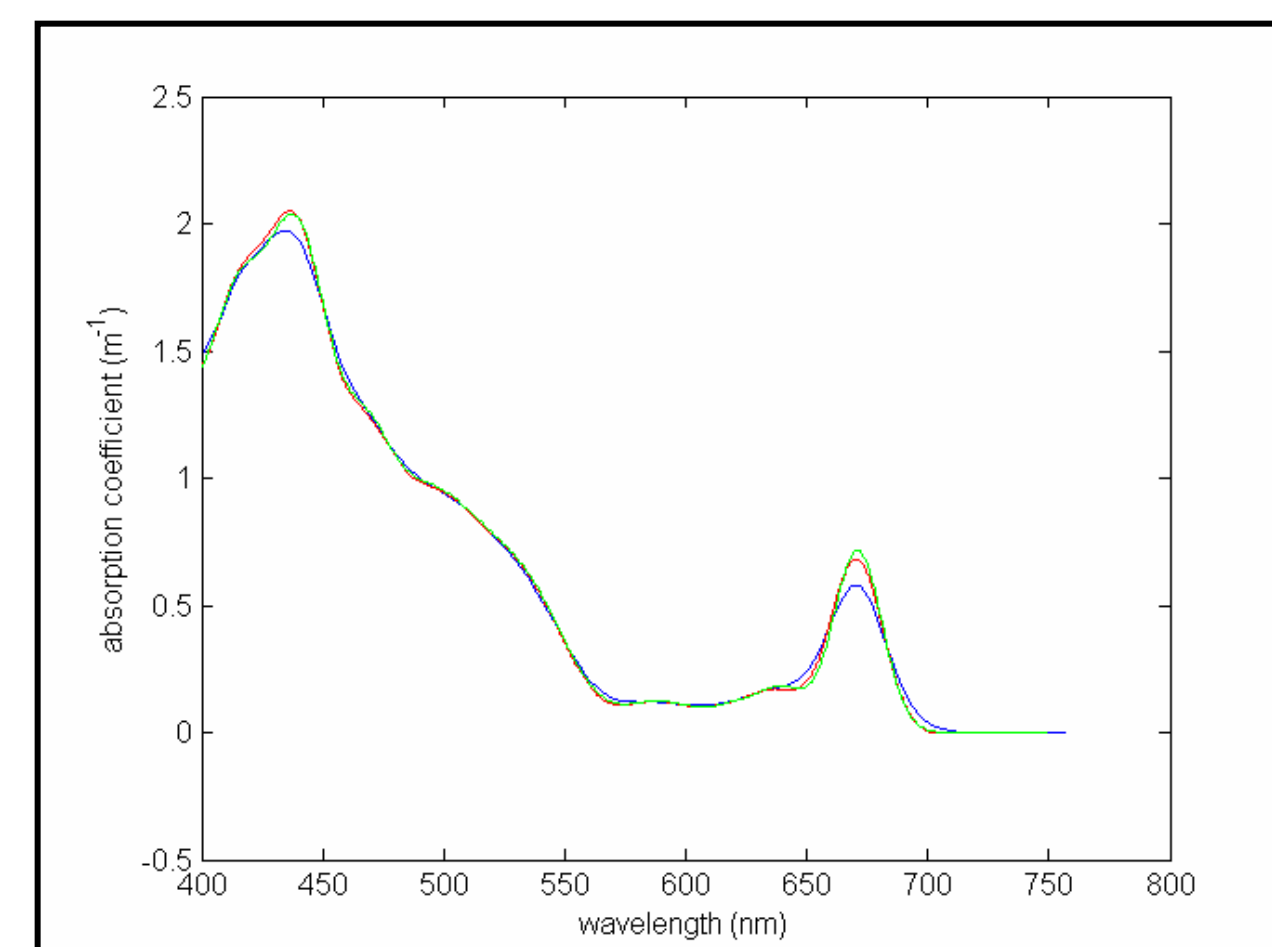


Figure 4. "Actual" (green), "measured" (blue), and corrected (red) absorption spectra for simulated green algae. The spectrum was modeled after absorption spectra found in Fig. 9.4 in Kirk (1994).

The correction very nicely recovers the original absorption spectrum. This works only for the relatively broad absorption peaks (and valleys), typically wider than 15 nm, that are found in naturally occurring phytoplankton assemblages.

## Gaussian components

The "actual" spectrum was simulated using multiple normal distributions (Bidigare et al., 1990; Hoepffner and Sathyandranath, 1991). As an example, the constituent normal distributions for the "actual" spectrum in Fig. 4 are shown in Fig. 5. This sort of construction is based on reality as absorption spectra in natural waters are due to a limited number of pigments with relatively wide absorption spectra. We modeled yellow matter by means of a normal distribution centered at 340 nm, with a very wide FWHM. The mathematical representation of one of the component normal distributions is:

$$D_i(\lambda) = A_i \exp\{-0.5[(\lambda - \lambda_{i0})/\sigma_i]^2\} \quad (4)$$

where  $A_i$  is the amplitude of the  $i^{\text{th}}$  component,  $\lambda_{i0}$  the central wavelength, and  $\sigma_i$  gives the width and is related to the FWHM by:

$$\text{FWHM} = 2.355\sigma_i$$

The total spectrum is then given by:

$$a(\lambda) = \sum_{i=1}^n A_i \exp\{-0.5[(\lambda - \lambda_{i0})/\sigma_i]^2\} \quad (5)$$

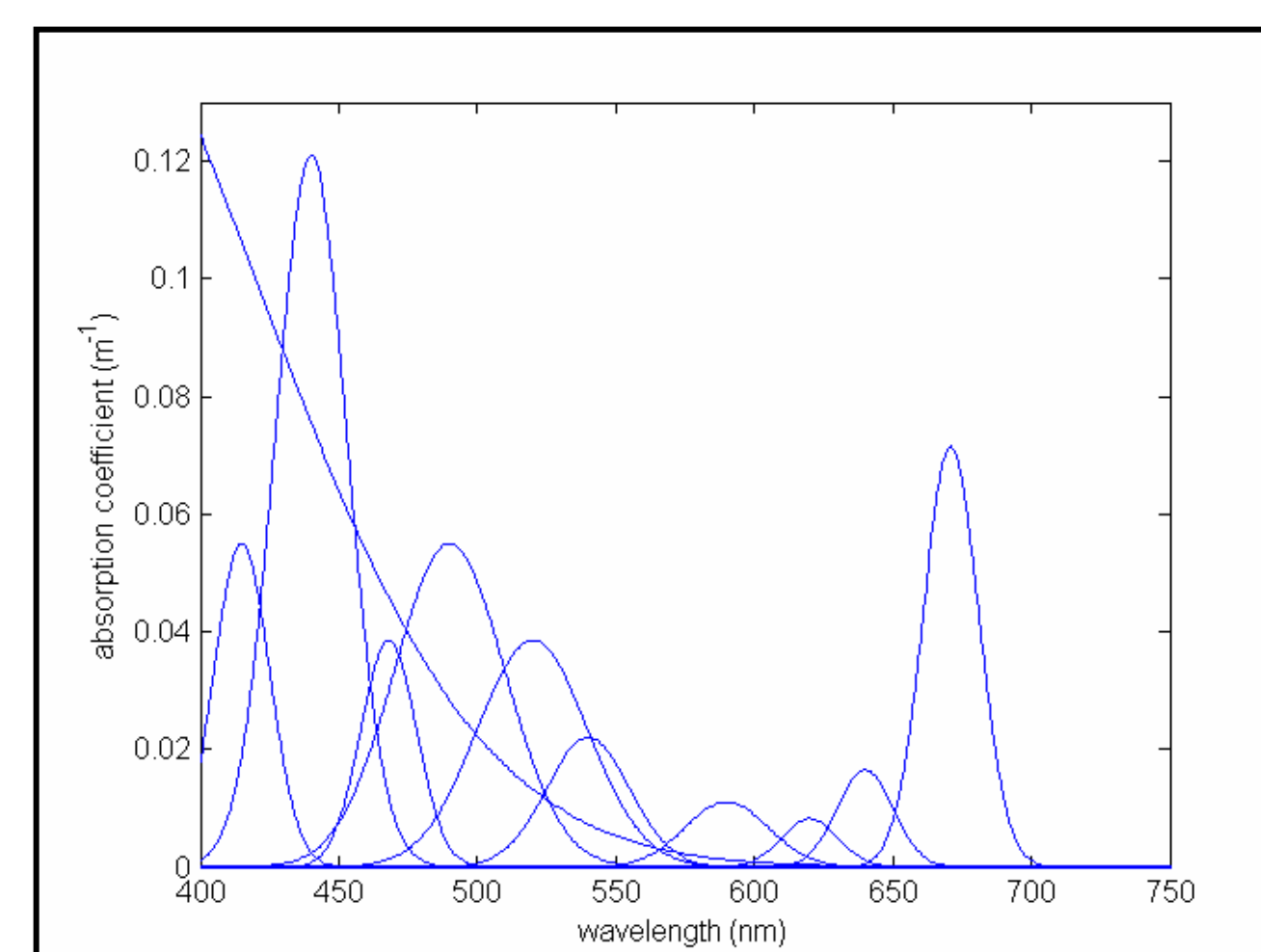


Figure 5. Constituent normal distributions used to generate the "actual" absorption spectrum in Fig. 4.

## Recovering constituent spectra.

In reality as well as in our model, the absorption spectra for particulates are made up out of a superposition of normal components, as in Eqs. 1 and 2. In order to recover the constituents we need to determine the parameters  $A_i$ ,  $\lambda_{i0}$  and  $\sigma_i$ . The second derivative displays maxima when the slope of the spectrum changes in a narrow wavelength band. Thus peaks, but also "bumps" are detected by the second derivative. By looking for maxima in the second derivative, we attempt to recover the central wavelengths  $\lambda_{i0}$  of the constituent normal distributions. Once we have found these central wavelengths we can set up a minimization routine that presupposes components with certain values for  $\sigma_i$ . Typically we choose two values, 10 and 15, although more components can be chosen. Minimization then determines the values for  $A_i$ . We can then add the components and see how well the scheme recovers the original spectrum. Fig. 8 shows an example for the corrected curve of Fig. 7. It is seen that the method does an excellent job of reconstituting the original spectrum. Clearly such a solution is not unique, but we hope to be able to extract with reasonable accuracy the contributions of the various pigments.

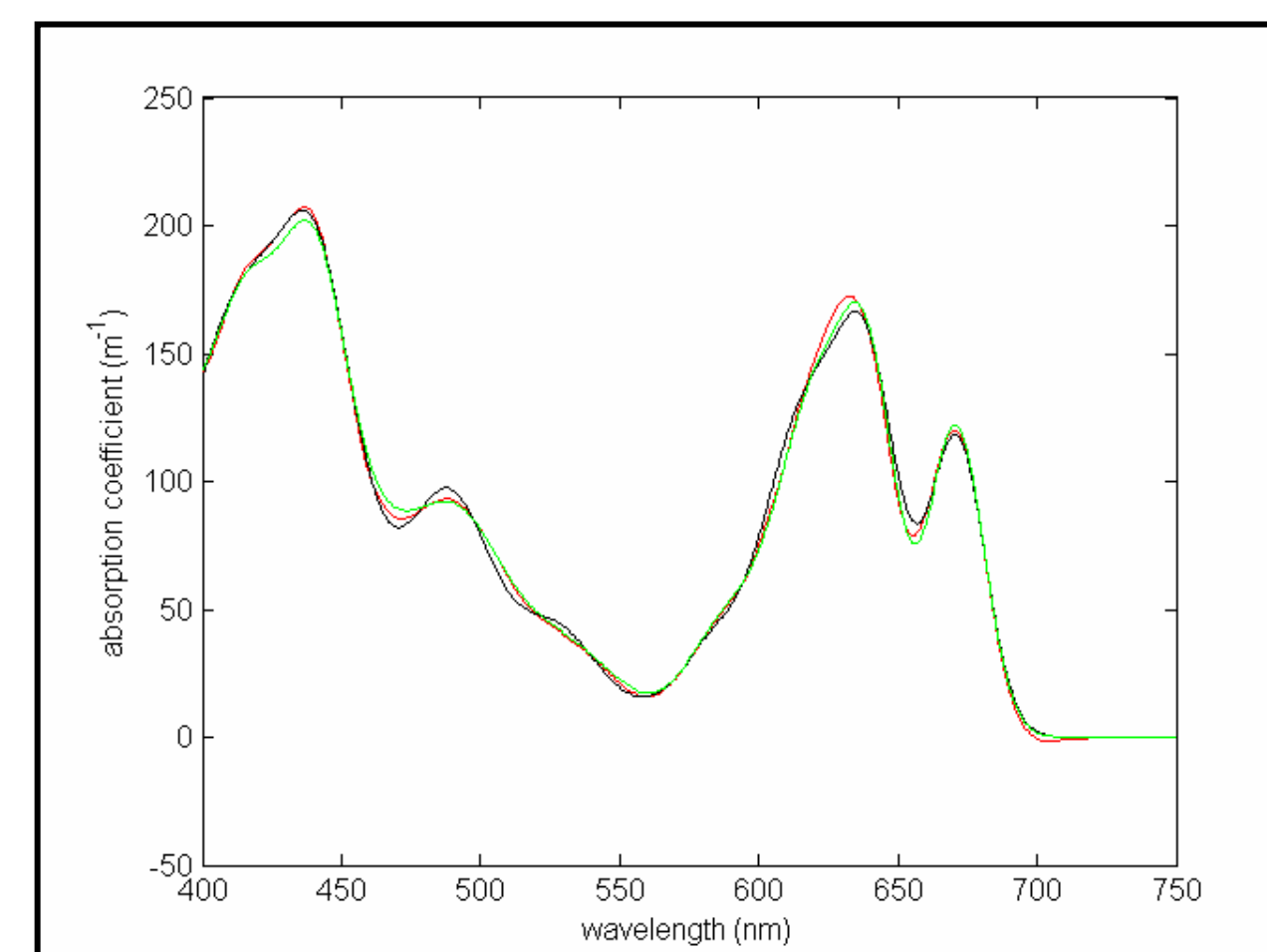


Figure 6. "Actual" absorption spectrum for blue-green algae (green curve), corrected spectrum (red) and reconstituted spectrum from normal components with central wavelengths calculated from the second derivative (black).

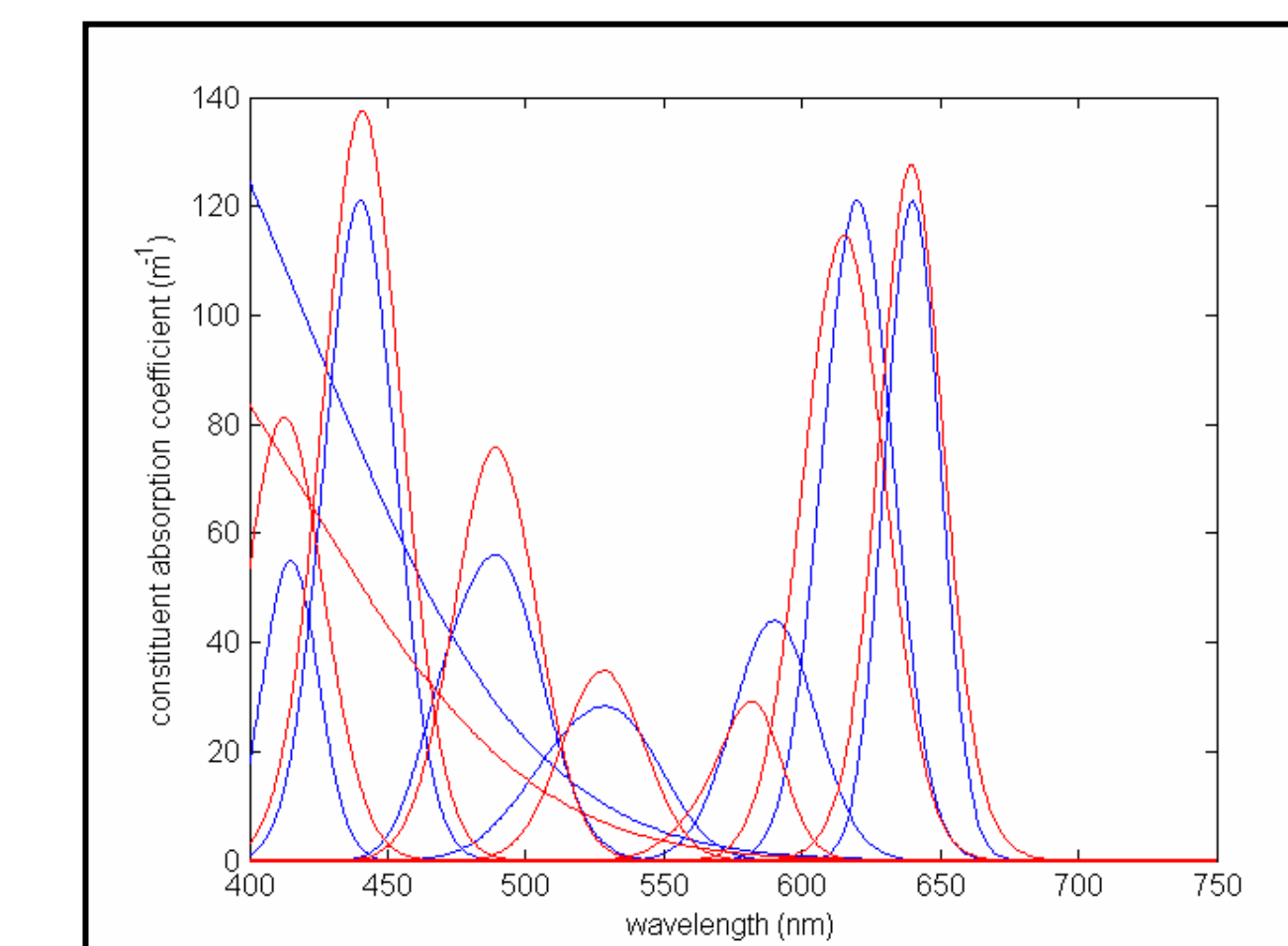


Figure 7. Components of the original "actual" blue-green algae absorption spectrum as in Fig. 6 (blue) and the reconstituted components (red). Minor components were summed.

## Analysis of Hawaii– Aloha ac-s data

The data shown below were taken at the Hawaii Ocean Time series Aloha site near 22.75°N, 158°W (approximately 100 km north of Oahu, Hawaii) on August 11, 2004. The data were obtained during two consecutive down and up profiles.

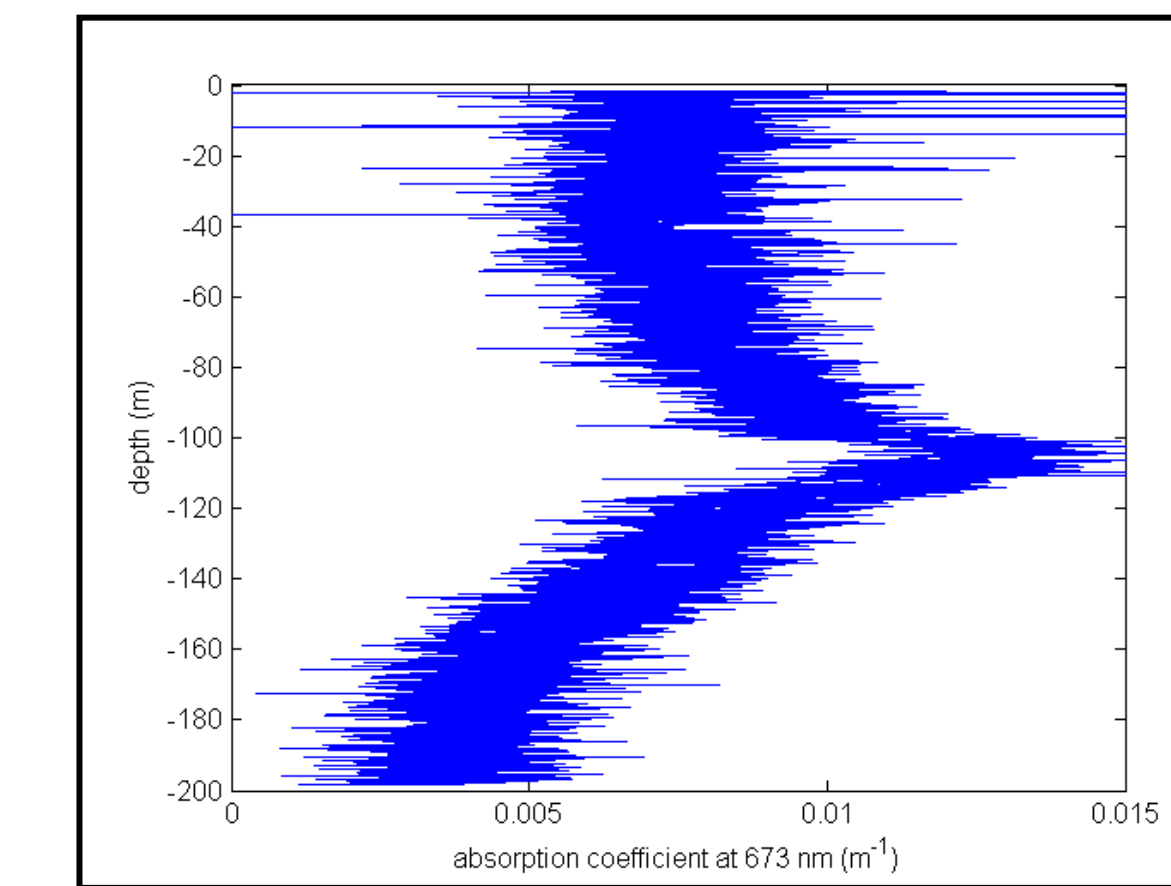


Figure 8. Two superimposed down and up temperature and salinity corrected profiles of  $a_{673}(673\text{nm})$  at the Hawaii– Aloha site. Note chlorophyll maximum near 100m as well as the extremely low values overall and the repeatability of approx.  $\pm 0.002 \text{ m}^{-1}$ .

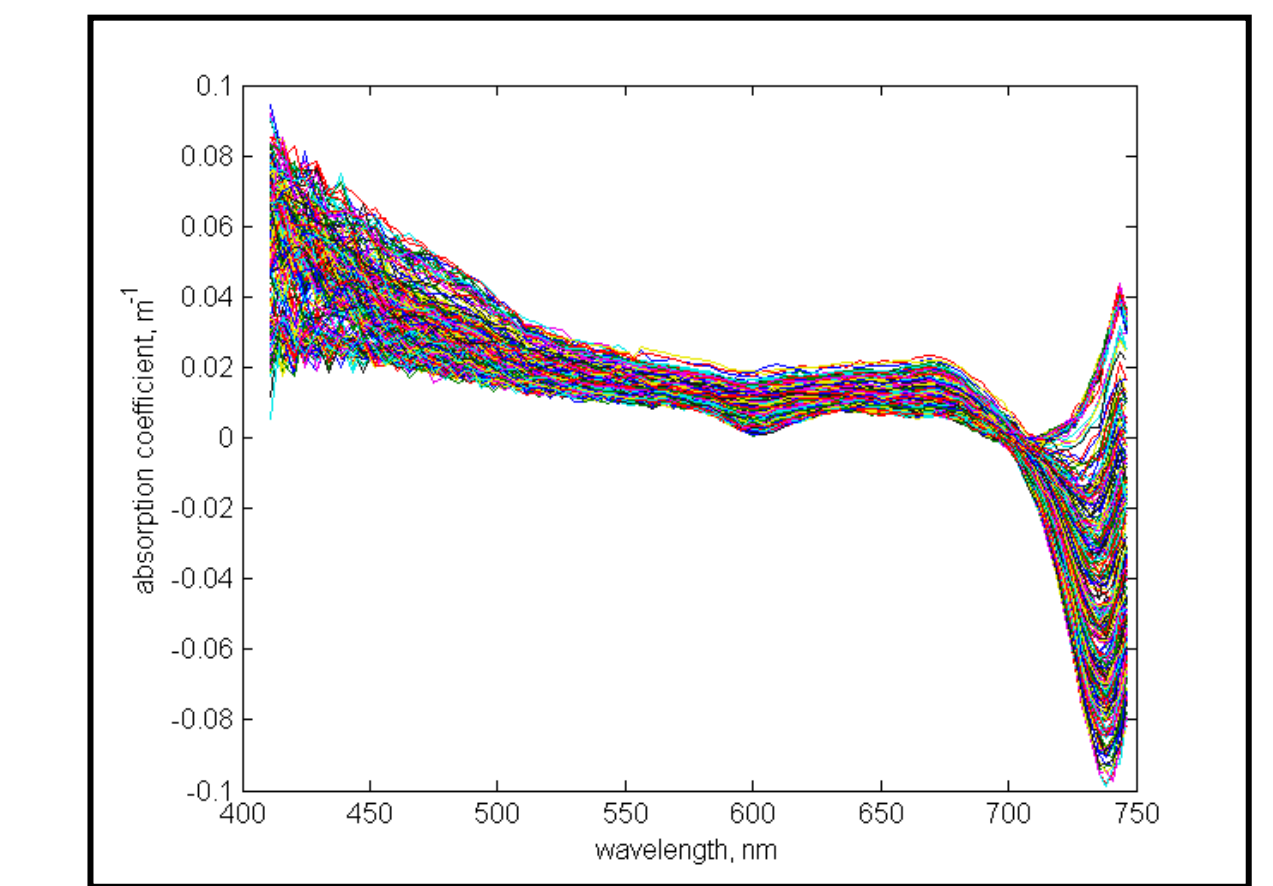


Figure 9. Raw ac-s absorption spectra from two consecutive down and up profiles. These are 7495 superimposed absorption spectra. There are temperature and salinity effects near 600 nm and in the infrared from 700 to 750 nm.

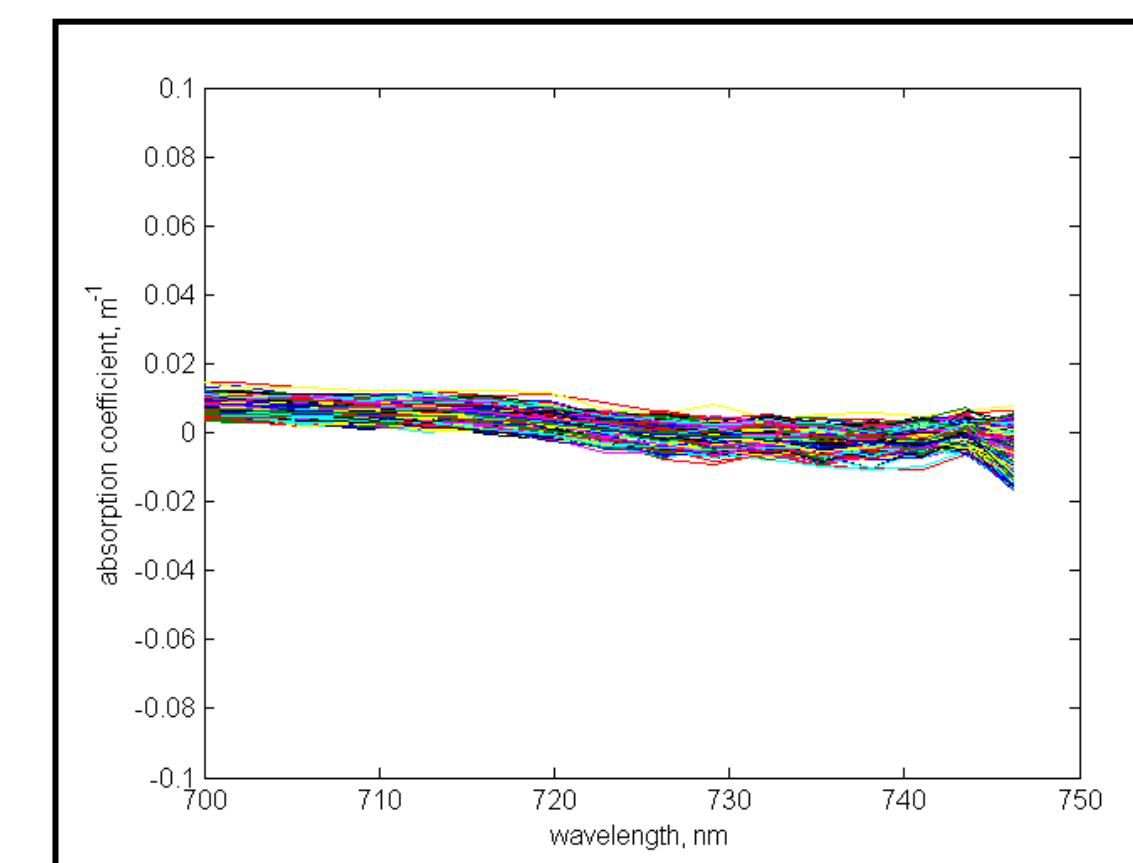


Figure 10. Temperature and salinity corrected absorption coefficients in the infra-red, measured at the Hawaii Aloha site.

These spectra were corrected using the  $\Psi_t$  and  $\Psi_s$  coefficients in Pegau et al, 1997 with a value added in the salinity correction at 733 nm. We set  $\Psi_s(733) = -0.00020$ . This is justified by recent observations by J. Sullivan (pers. comm., see poster at this meeting). Intermediate values were interpolated. The salinity corrections are important and on the same order as the temperature corrections. This is because the instrument is calibrated in fresh water. The salinity difference between the lab and the ocean is thus large.

Note that most values in the 720– 750 nm region are now within  $\pm 0.005 \text{ m}^{-1}$  of zero.

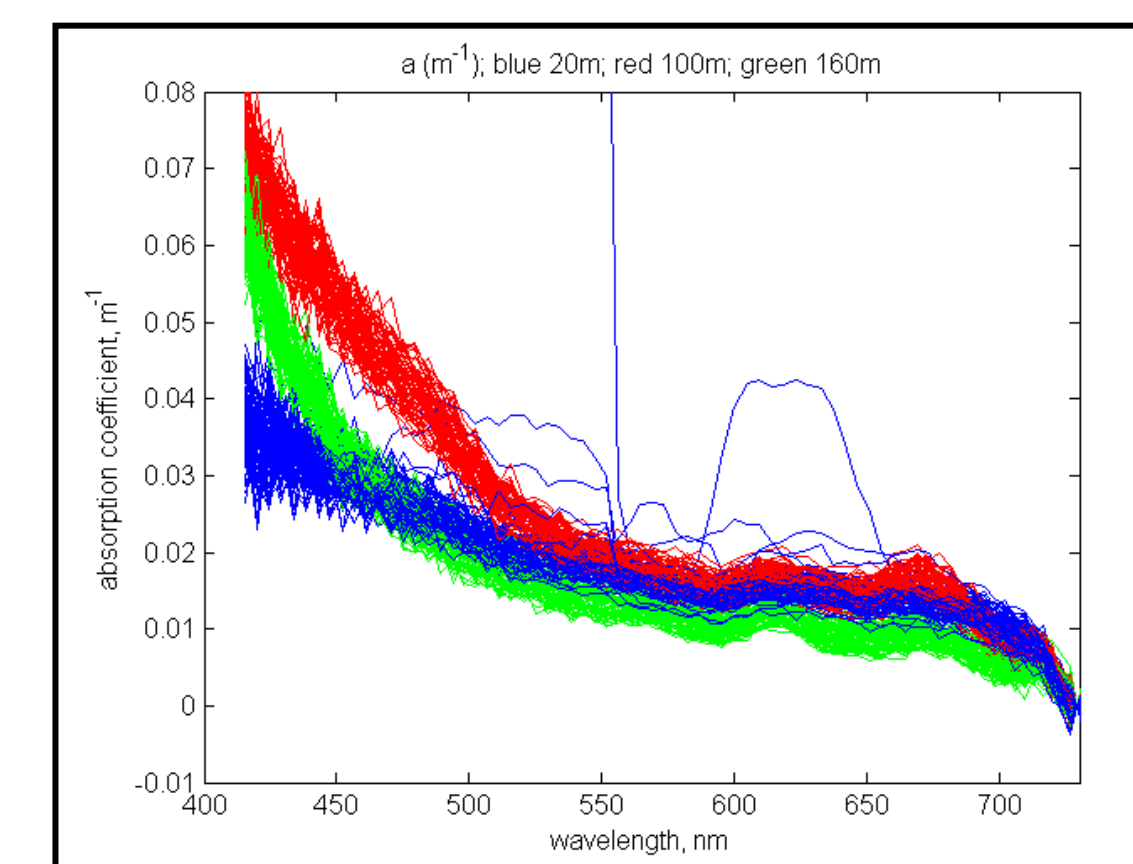


Figure 11. Corrected absorption spectra at 20 (blue), 100 (red), and 160 (green) m depth (1m depth bins). The chlorophyll maximum is near 100m depth, and 20m is within the mixed layer.

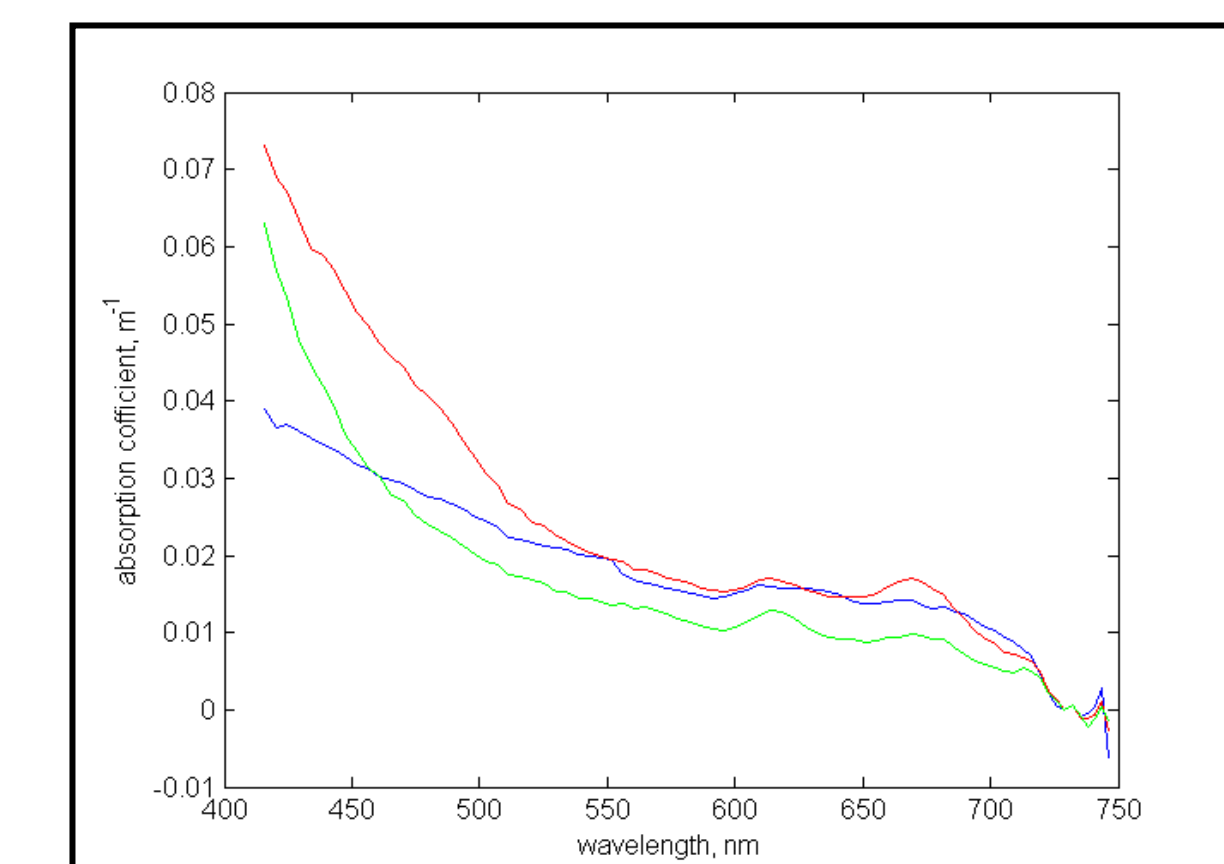


Figure 12. Average absorption spectra for each depth shown in Figure 11.

Figs. 11 and 12 demonstrate that the instrument is repeatable, at least in the short term, to within  $\pm 0.005 \text{ m}^{-1}$ , even in the blue. Even though the absorption values are quite low, the absorption spectra in the mixed layer (20m), at the chlorophyll maximum (100m) and below the chlorophyll maximum (160m) have different spectra. The overall signal is largest at 100m, as this is the depth of the chlorophyll maximum. At 100m, we also see maximum absorption at 672nm, whereas at the other depths, the maximum absorption occurs at around 620nm. Kirk (1983) shows that for blue-green algae there is a maximum absorption peak at 620 nm, with a lesser peak at 672. An example of a green alga is *Synechocystis*. The data from 100m also clearly shows a bulge at 480 nm, indicating the presence of ancillary pigments, only weakly present at 20m and not at all at 100m

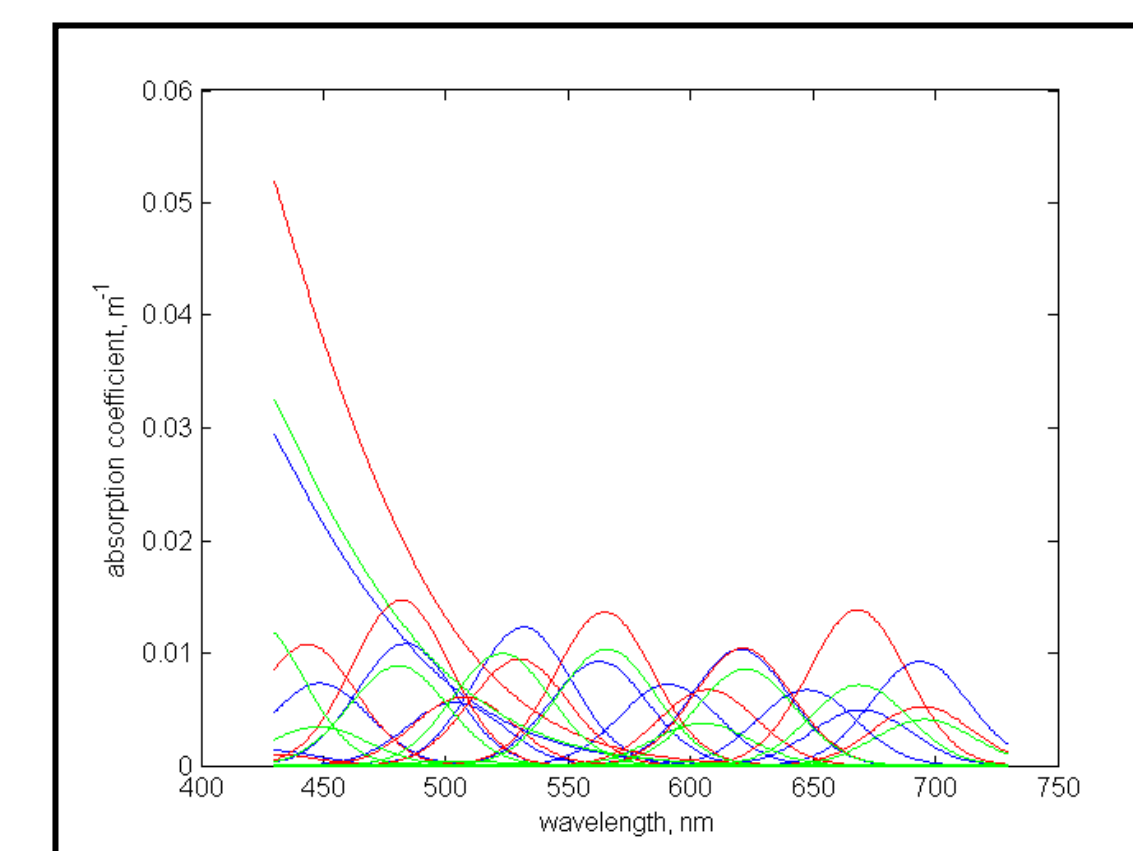


Figure 13. The Gaussian components for the 20m (blue), 100m (red) and 160m (green) average absorption spectra.

## Conclusions

The ac-s data can be corrected for the width of the filter factors provided the absorption peaks are relatively wide (Order of 10nm). In the extremely clear waters north of Hawaii, the ac-s showed a remarkable ability to distinguish minor shapes and concentrations in spectra of the absorption coefficient. The spectral dependence of pure water on temperature and salinity must be further studied in the near IR, in order to make sure of the corrections. The instrument appears to be operating well within its specifications. Repeatability was better than  $\pm 0.002 \text{ m}^{-1}$ . Accuracy appears to be within  $\pm 0.005 \text{ m}^{-1}$ .

Even in this extremely clear and therefore challenging environment, spectra at different depths showed different constituent concentrations, both by analysis of the spectra themselves, as well as by Gaussian component analysis.

## References

- Bidigare et al., 1990, Ocean Optics X, Proc. SPIE 1302, 290-302.
- Hoepffner and Sathyandranath, 1991, Mar. Ecol. Prog. Ser., 73(1), 11-23.
- Kirk, J. T. O., Light and Photosynthesis in Aquatic Ecosystems, Cambridge Univ. Press. (1983)
- Moore, Zaneveld, and Kitchen, 1992, Proc. SPIE 1750, 330-337.
- Pegau, Gray, and Zaneveld, Absorption of visible and near-infrared light in water: the dependence on temperature and salinity. *Applied Optics* 36(24) 6035-6046 (1997)
- Zaneveld, Kitchen, and Moore, Scattering error correction of reflecting tube absorption meters *Ocean Optics XII*, S. Ackleson, Ed., Proc. SPIE Vol. 2258, 44-55 (1994)

## Acknowledgments

Development of the instrument was partly supported through NASA SBIR funding. The experimental effort was partly supported through the National Oceanographic Partnership Program.